J Mater Sci (2022) 57:10407–10424

Polymers & biopolymers

Semitransparent films from low-substituted carboxymethylated cellulose fibers

Yichen Liao[1], Nur Alam[2], and Pedram Fatehi[1,2,*]

[1] Chemical Engineering Department, Lakehead University, 955 Oliver Road, Thunder Bay, ON P7B 5E1, Canada
[2] Biorefining Research Institute, Lakehead University, 1294 Balmoral Street, Thunder Bay, ON P7B 5E1, Canada

Received: 18 January 2022
Accepted: 21 April 2022
Published online: 18 May 2022

ABSTRACT

Cellulose-derived films have received attention for possible use in the packaging industry. However, the poor mechanical properties of the biofilm are the main concern. This study aims to mildly carboxymethylate cellulose fibers and esterify the generated carboxymethylated cellulose fibers (CMF) for film production. The physicochemical alteration of cellulose fibers via carboxymethylation and esterification was confirmed by means of solid-state carbon NMR, FTIR, and XPS analyses. The carboxymethylation of cellulose fibers impacted their surface morphology and fiber length dramatically. The results confirmed that the carboxymethylated cellulose fibers (CMF) with a 1.2 mmol/g carboxylate group generated films with the highest mechanical properties. The higher degree of carboxymethylation tended to reduce the mechanical properties but improved the optical properties of the CMF film as smaller CMF could scatter light more effectively. The use of acetic acid (3 wt%) was crucial in the esterification of CMF to generate CMF film with the highest tensile strength (60.8 MPa), but a higher concentration of acetic acid would impair the mechanical properties of the film. The great tensile strength of the CMF derived film (60.8 MPa) and the relatively uncomplicated fabrication procedure of CMF films are promising for some applications, such as bags and agriculture uses. However, the water uptake of the CMF films was relatively high (3–4 g/g), and further research needs to address this challenge.

Handling Editor: Stephen Eichhorn.

Address correspondence to E-mail: pfatehi@lakeheadu.ca

https://doi.org/10.1007/s10853-022-07262-0

GRAPHICAL ABSTRACT

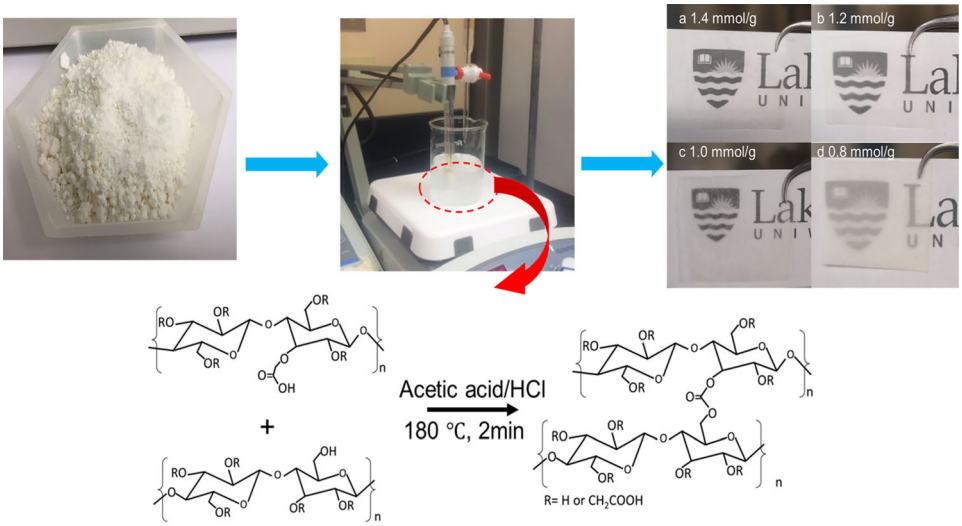

Introduction

Cellulose can be generated from many resources, such as wood, seed fibers, peel fibers, bast fibers, grasses, marine animals, algae, fungi, and bacteria [1–5]. This biomaterial exhibits desired properties, such as biodegradability, renewability, high strength, and biocompatibility, which are required for many applications [6]. Cellulose has attracted tremendous attention in the areas of reinforced polymer products [7], absorbent materials [8], sensors [9, 10], and packaging materials [11]. Cellulose exists in fiber bundles naturally in lignocellulosic biomass [12], which is not suitable for film production. The conventional fibrillation strategies of cellulose derivatives, such as grinding, ultrasonication, extrusion, high-pressure homogenization refining, and ball mailing are energy-intensive [2, 5, 13, 14]. To reduce the energy cost, chemical pretreatments are suggested as other alternative routes. In this case, the compatibility of cellulose fibers with other materials may also be improved via a chemical treatment, which would facilitate the use of cellulose fibers in film productions.

Numerous chemical modification strategies were applied to cellulose fibers including oxidation and etherification [2, 14]. Carboxymethylation is a versatile surface modification strategy that can improve the water solubility of cellulose fibers by introducing carboxymethylated groups on their surface. Carboxymethylation can also improve the electrostatic repulsion between cellulose molecules and thus reduce the hydrogen bonding development between cellulose molecules [4, 15, 16]. Thus, this process would presumably reduce the intensity of mechanical grinding to obtain thinner cellulose fibrils. Furthermore, carboxymethylation is the most economical and facile method compared with more complicated 2, 2, 6, 6-tetra-methyl piperidine-1-oxyl radical (TEMPO) and periodate-chlorite oxidation strategies to introduce surface charges to cellulose fibers [8]. Numerous studies on the carboxymethylation of cellulose fibers were carried out to optimize the reaction conditions for increasing the production yield and efficiency [17–24]. In this regard, the previous studies showed that a high degree of carboxymethylation reduced the mechanical and optical properties of cellulose fibers, which would hinder their application in the packaging industry [4, 5, 9, 24, 25]. In the present work, as the first objective, we generated carboxymethylated cellulose fibers with a low substitution degree so that extensive fibrillation can be avoided while the carboxymethylated fibers could have a reasonable entanglement degree [4, 5, 15, 17, 26, 27].

Cellulose derivatives have been utilized for the preparation of edible film in packaging applications. The criteria of bioplastic in the packaging industry include transparency, mechanical properties, and water barrier properties. Cellulose-based films, such as cellophane, methylcellulose (MC), hydroxypropyl cellulose (HPC), carboxymethylated cellulose (CMC), and hydroxypropyl methylcellulose (HPMC) films, were suggested for packaging applications due to their transparency and odorless characteristics [28–31]. However, the challenge of utilizing these films is their weak mechanical properties making them non-competitive with the other petroleum-based products [32–36]. To improve the barrier and mechanical properties of cellulose-based films, various methodologies, such as crosslinking, blending, grafting, copolymerization with polymers (protein, lipid, polysaccharide, and polyvinyl alcohol), were suggested [37–40]. However, the low compatibility of some polymers with cellulose fibers may hinder their fabrication process. Also, the toxicity of some of these polymers, such as formaldehyde and acrolein, is a primary concern for the food packaging application [41]. Interestingly, Borůvková and coworkers studied the esterification of carboxylic acid and hydroxyl groups of cellulose fibers [42]. The second objective of this work was to assess how the esterification of carboxymethylated cellulose fibers would improve the properties of films produced from them.

In the past, cellulose-based films, such as regenerated cellulose and nanofibril cellulose-based films, were produced and they had high mechanical properties, light transparency, and good barrier properties. However, the production process of these cellulose derivatives is high, which makes them less appealing for general use. These products were recommended to be used for high-end applications, such as electric devices, sensors, and biomedical devices [43–45]. Unlike these cellulose derivatives, the CMF-based films reported in this work utilize cellulose fibers that are less expensive than those cellulose derivatives for value-added applications.

In this work, cellulose fibers were first carboxymethylated to different degrees, and then cellulose-based films were produced from carboxymethylated fibers. The carboxymethylation reaction and fiber properties, as well as film properties and film performance, were assessed comprehensively using advanced methods, such as Fourier transform infrared spectroscopy (FTIR), X-ray photoelectron spectrometry (XPS), solid-state ^{13}C nuclear magnetic resonance (NMR), scanned electron microscopy (SEM), UV–visible spectrophotometry, water uptake, particle size distribution (PSD), tensile strength, and Young's modulus.

Materials and methods

Materials

Bleached softwood kraft pulp was provided by a kraft pulp mill in northern Ontario, Canada. Sodium hydroxide, monochloroacetic acid (MCA), isopropyl alcohol, IPA (> 99%), acetic acid (> 99%), and sodium chloride were obtained from Sigma-Aldrich and used as received. Hydrochloric acid (36.5%) was also obtained from Sigma-Aldrich and diluted to 0.1 M before use. Ethanol (95%) was obtained from Fisher Scientific Company.

Preparation of carboxymethylated cellulose fibers (CMF)

The carboxymethylation of the pulp was conducted as described in the literature on the carboxymethylation of cellulose [20, 22]. A 4 g sample of bleached softwood pulp was added to 44 g of IPA along with 1.25 g of sodium hydroxide solution at 4 °C for 1 h at a stirring rate of 500 rpm. Then, they were mixed with different amounts of sodium chloroacetate (MCA) at 60 °C for 2 h. After the reaction, the pulp slurry was washed 3 to 4 times with 70–100% ethanol. The carboxymethylated pulp was dried at 60 °C and stored at room temperature for further use. This product is denoted as carboxymethylated fiber (CMF), and its production yield was determined with respect to the ratio of the dry weight of the CMF product after carboxymethylation and the dry weight of the initial pulp. The reaction yield of CMF was calculated following Eq. (1)

$$\text{Reaction yield} = C_{[\text{coo}-]} \times W_{\text{Pulp}} \div N_{\text{MCA}} \times 100\% \quad (1)$$

where $C_{[\text{COO}-]}$ is the carboxylate group content (mmol/g) of carboxymethylated cellulose, W_{Pulp} is the weight (g) of pulp used in carboxymethylation reaction, and N_{MCA} is the mole of sodium chloroacetate, MCA (mmole), involved in the carboxymethylation reaction.

Determination of carboxylate content

The conductometry titration was used for measuring the total carboxylate group of CMF using an automatic conductometer (Metrohm 856 Titrado, Switzerland) according to the method described by Yang and coworkers [46]. Briefly, 0.11 g of CMF and 2.5 mL 0.02 M sodium chloride were dispersed in 120 g of deionized water while stirring at 300 rpm. The suspension was titrated with 0.05 M NaOH. The content of the carboxylate group was then determined.

CMF fibrillation

The CMF fibrillation was conducted by thermal and shearing forces as follows: CMF was well dispersed at 350 rpm with a magnetic stirrer in deionized water in a 250 mL glass flask to achieve a 150 mL of 2 wt% suspensions. The pH of the suspension was adjusted to 9 by adding 1 M of sodium hydroxide solution. The suspension was then heated at 90 °C for 2 h.

CMF film curing and casting

The CMF was changed from fiber bundles to individual cellulose fibers or smaller fiber debris under the shear force after the process stated in the previous section. The film curing step was the continuation of the previous section and conducted in the same glass flask stated previously. The pH of CMF suspension was adjusted to 3.4 using acetic acid or 1 M HCl, which caused the protonation of CMF fibers. Then, different amounts (5 wt%, 4 wt%, 3 wt%, 2 wt%, and 1 wt%) of acetic acid, as a weak acid with insignificant damaging effect or HCl were added to the CMF suspension based on the weight of the dried CMF sample, and the system was stirred at 500 rpm for another 1 h. Afterward, the CMF suspension was cast onto a plastic plate (100 mm diameter) and vacuum-dried using a vacuum oven at 60 °C overnight. The collected CMF film was then cured in a muffle furnace at 180 °C for 2 min. The cured CMF film was stored in a plastic bag at room temperature for further use.

Fourier transform infrared spectroscopy (FTIR)

The Fourier transform infrared (FT-IR) spectra of the cellulose fibers, CMF, and CMF film were recorded with an attenuated total reflectance (ATR) of a Tensor 37 spectrometer (Bruker, Germany) with a scanning range of 600–4000 cm^{-1} at a scanning speed of 32 scans/s with a resolution of 4 cm^{-1}.

X-ray photoelectron spectrometry (XPS)

The XPS analysis of the cellulose fibers, CMF, and CMF film was performed using a photoelectron spectrometer (XPS, Escalab 250XL+, Thermofisher Scientific, USA). All the samples were dried in a 60 °C oven overnight before the XPS measurement. In this experiment, 10 mg of dried samples were used directly. Spectrum was recorded using a monochromatic Al KαX-ray source (1486.7 eV) operating at 15 kV (90 W) in a transmission mode with a pass energy of 40 eV for the ROI region, and 80 eV for the survey region. The high-energy resolution spectra were acquired using an energy analyzer operating at a resolution of approximately 0.65 eV and pass energy of 187 eV. The binding energy scale was calibrated by the C 1 s line of aliphatic carbon, which was set at 285 eV. Full-spectra, narrow high-energy resolution spectra, elemental compositions, and functional groups were assessed using ESCApe software.

Solid-state 13C nuclear magnetic resonance (NMR)

The ^{13}C NMR analysis of cellulose fibers, CMFs, and CMF films was performed using 60 mg of previously dried samples (60 °C, 24 h). The dried samples were directly packed into a 4 mm cylinder MAS rotor (Bruker, German) and compressed by a metal packer. The rotor was then sealed with a 4 mm MAS Kel-F rotor cap (Bruker, German) for the NMR measurement. The solid-state ^{13}C NMR spectra of all samples were recorded on nuclear magnetic resonance spectroscopy (UNITY INOVA^{TM}, 500 MHz, Varian, Inc.) with a 4 mm MAS rotor (Bruker, German) in a total of 64 scans per sample at 25 °C and a 2.05 s acquisition time, a 90 ° pulse, and 1.00 s of relaxation delay time.

Particle size distribution

The particle size distributions of cellulose fibers and CMF prepared in the previous section were studied comprehensively by a Mastersizer Micro Plus 3000 (Malvern Instruments, Worcestershire, UK) in the

range of 0.01 μm and 3300 μm. The samples were dispersed into deionized water by magnetic stirring at the speed of 450 rpm to obtain adequate dispersed suspension before measuring the particle sizes.

Optical properties

The optical transmittance of CMF films was measured using a Varian UV–visible spectrophotometer (Cary 50, USA). The background spectrum was obtained by measuring an empty sample holder, and the film was then placed on the holder for measurement. The spectra were acquired from 200 to 900 nm with a data interval of 5 nm. Transmittance ($T\% = I/I_0$, where I and I_0 were the intensities of emergent and incident radiation, respectively) was used for defining the transparency of the CMF film. To compare the influence of different conditions on the transparency of films, the optical transmittance values were obtained at 600 nm, which is the approximate average wavelength in the visible light region [46].

Tensile strength

The tensile strength and Young's modulus of films were measured using a tensile tester (Instron Mini 44, US) with a 500 N load cell in a standard conditioned room (temperature 22.2 ± 0.6 °C, relative humidity 50 ± 2%). Films were cut into strips (10 mm wide × 50 mm long), which were stretched at a crosshead speed of 1 mm/min with a specimen gauge length of 10 mm. Each result was reported based on at least three measurements.

Scanned electron microscopy (SEM)

The CMF and CMF films were coated with gold for the SEM observation. The SEM images of the gold-coated samples were acquired by a scan electron microscope (Hitachi SU-70, Japan) under the condition of an accelerating voltage of 5.0 kV under the vacuum (10^{-4}–10^{-3} Pa) with the magnification of 100× to 500×.

Water uptake

Initially, the CMF films were dried in the oven at 105 °C for 1 h before water uptake measurement. The dried films were then immersed in the deionized water for 24 h. After the submersion period, the immersed films were removed and swept with a paper towel. The water uptake of the samples was recorded according to Eq. 2:

$$(\mathrm{WU} = W_{\mathrm{immersed}} - W_{\mathrm{initial}}) \div W_{\mathrm{initial}} \quad (2)$$

where WU is water uptake (g/g) of CMF films, W_{immersed} is the weight (g) of immersed film, and W_{initial} is the dry weight (g) of the CMF film before immersing into water.

Results and discussion

Carboxymethylation of cellulose fibers

The carboxymethylation of cellulose fibers was performed using sodium chloroacetate as a carboxylate group donor. Under alkaline conditions, NaOH will activate cellulose fibers, which will then react with monochloroacetic acid or its sodium salt to form carboxymethylated cellulose fibers [47].

The CMF samples with different carboxylate group contents are shown in Table 1. As the reaction proceeded (Figure S1 in the supplementary material), MCA could substitute the hydroxyl group of the cellulose fibers. The maximum carboxylate content of the CMF sample was 2.1 mmolg^{-1}. The reaction yields of the carboxymethylation were between 42.3 and 66.5%, and the product yields of CMFs ranged from 105.8 to 110%. Unlike the TEMPO-oxidation (C6 hydroxyl groups) and periodate oxidation (C2 and C3 bond), the carboxymethylation of cellulose fibers could occur randomly on the C2, C3, and C6 bonds of the glucose ring. Carboxymethylation may also facilitate the breakage of hydrogen bonding within cellulose structure and thus enlarge the gap between the cellulose fiber bundles, which would promote the separation of fibers to micro or nanofibers [25, 48]. As stated in the literature, altered factors, e.g., temperature, time, solvent type, NaOH, and MCA concentrations, would influence the carboxymethylation reaction [20, 22, 49, 50]. In this study, the amount of introduced carboxylate group was correlated with the addition of MCA. The more MCA involved in the reaction, the more carboxylate groups were introduced onto cellulose fibers. However, sample 1 exhibited a relatively low reaction yield (42.3%). One possibility for such results could be that a large amount of MCA would facilitate the side reaction of the carboxymethylation (Figure S2 in the

Table 1 Preparation of CMF from the pulp in an aqueous alkaline solution in the presence of different amounts of MCA (temperature 60 °C for 3 h)

Sample	Pulp (g)	IPA (g)	NaOH (g)	MCA (mmol)	Carboxylic content (mmol/g)	Reaction yield (%)	Product (CMF) yield (%)
1	4	44	1.25	19.8	2.1	42.3	113.6
2	4	44	1.25	8.4	1.4	66.5	110.0
3	4	44	1.25	7.2	1.2	67.1	108.5
4	4	44	1.25	6.3	1.0	63.4	107.0
5	4	44	1.25	5.5	0.8	58.5	105.8
6	4	44	1.25	3.9	0.5	51.0	102.6

supplementary material), which would reduce the reaction yield [18].

Particle size and morphology analysis

As seen in Fig. 1a, b, carboxymethylation did not change the surface morphology of fibers. After fibrillation via heating and stirring, in the curing step, however, the CMF delaminated to thinner fibers (Fig. 1c). An analogous result can be found in the particle size distribution results of CMF as shown in Fig. 2.

The mass of smaller fibers increased with the introduction of more carboxylate groups on CMF (Fig. 2), leading to a reduction in the median diameter of CMFs from 13.2 μm ([COOH] = 0.8 mmol/g) to 2.91 μm ([COOH] = 1.4 mmol/g), which is similar to the results reported in the past [51]. However, the existence of some fiber fragments after heating and stirring in the casting and curing step (Fig. 1c) indicated the incomplete liberation of fibers [52]. Those fiber fragments contributing to the proportion of fibers with a length smaller than 1 μm were generated from the scission of fibers due to the shearing force or peeling reaction [53, 54]. Meanwhile, with more carboxylate groups participating in the reaction, the reduction in the fiber length might be intensified due to the elevation in the fiber breakage [51]. According to Nechyporchuk and coworkers, the fiber delamination could be accelerated by mechanical force [2]. Compared to other studies that combined chemical modification with conventional mechanical processes [1, 2, 5, 14, 15, 27, 55], our study employed

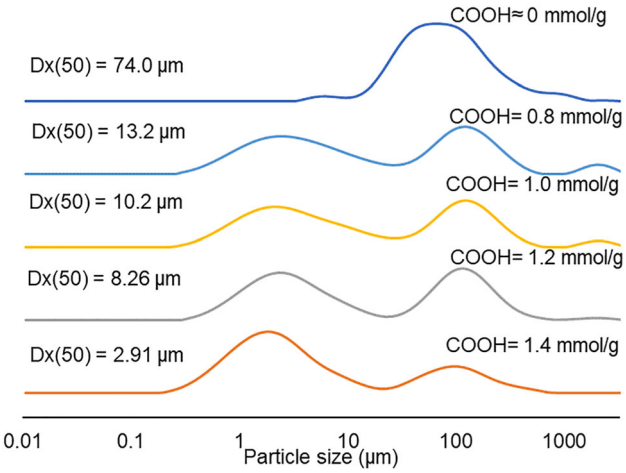

Figure 2 Particle size distribution of CMFs after heating and stirring with different carboxylate group contents.

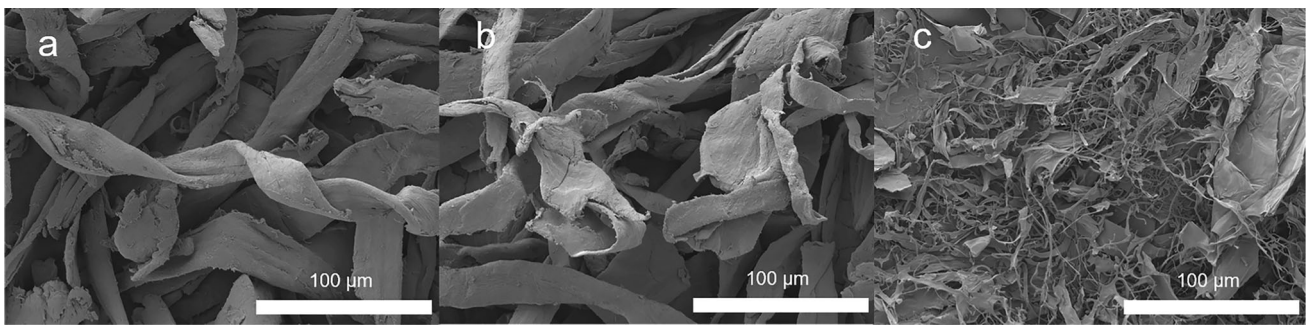

Figure 1 SEM images of cellulose fibers **a** before modification, **b** after modification (to have 1.2 mmol/g carboxylate group) and **c** after heating and stirring in the curing step.

lower intensity shear force (e.g., magnetic stirring) than those reported earlier, e.g., high-pressure homogenizer (60 MPa) or grinder (1500 rpm) [49, 51] to treat carboxymethylated cellulose fibers, which may further reduce the energy consumption of the proposed process for the carboxymethylation of cellulose fibers.

Esterification of CMF

Generally, the esterification of cellulose is an acylation process that could employ carboxylic acid, carboxylic acid anhydrides, or acid chlorides as acylating agents [56]. According to Wang and coworkers, the hydroxyl groups in anhydroglucose unit (AGU) of cellulose can take part in an esterification reaction [57]. Thus, the carboxymethylated cellulose has the potential for reacting and thus crosslinking with cellulose polymer chains as acylating agents via esterification. Borůvková and coworkers also stated that the crosslinking of carboxymethylated cellulose could occur due to the presence of hydroxyl and carboxylate groups on the fibers [42]. However, the low reactivity of carboxylic acid required either acid catalysis or thermal curing to activate the esterification reaction [56–58]. In our study, we employed acetic acid and HCl as catalysts during the film fabrication and cured CMF at 180 °C for 2 min. The scheme of esterification, i.e., self-crosslinking, of CMFs is shown in Figure S3 in supplementary material files. To confirm that the esterification successfully occurred between CMFs; the FTIR, XPS, and NMR analyses of the samples were carried out.

Figure 3 shows the solid-state ^{13}C NMR spectra of the CMF film, CMF, and cellulose fibers. The cellulose fibers, CMF, and CMF film showed similar peaks in the regions of 60 and 105 ppm, which would represent the carbon of the cellulose backbone. In detail, most of their carbon atoms exhibited signals at 61–63.5 (C6), 73.4 (C2, 3, 5), 80–88 (C4), and 103.5 (C1) ppm [59–61]. A new peak showed at 176.5 ppm, which corresponded to the carboxylate group (C7), and revealed that the carboxymethylation occurred on cellulose fibers [59, 62, 63]. Furthermore, the sharp carboxylate peak of CMF at 176.5 ppm was found to be slightly broadened toward the up-field region in the spectrum of CMF film. This is the result of the appearance of a new peak that corresponds to the carbonyl group at 173.2 ppm overlapping with the

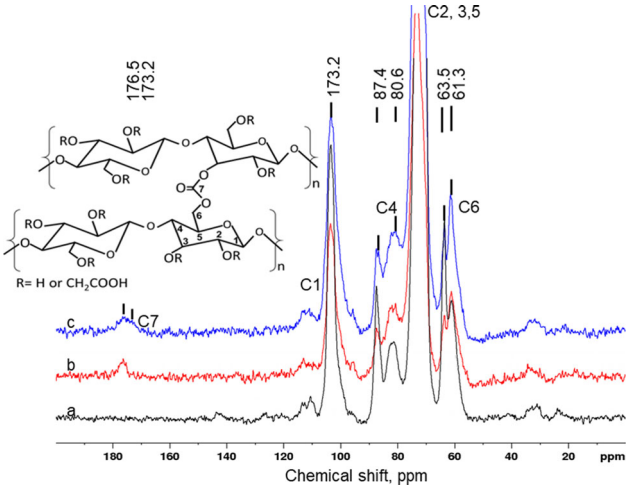

Figure 3 Solid-state ^{13}C NMR of **a** Cellulose fibers, **b** CMF, and **c** CMF film.

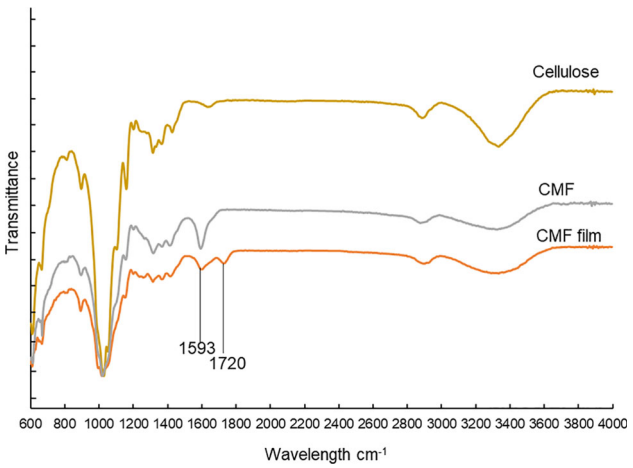

Figure 4 FT-IR transmittance spectra of **a** Cellulose fibers, **b** CMF, and **c** CMF film.

peak at 176.5 ppm [64, 65] and indicating the esterification occurrence between CMFs.

The FTIR spectra of cellulose fibers, CMF, and CMF film are shown in Fig. 4. In the infrared spectra, all samples exhibited similar absorption peaks. The bands at 3340 and 2905 cm^{-1} for all cellulose fibers, CMF, and CMF film correspond to the presence of the stretching vibrations of O–H and C–H, respectively [18]. The peak at 3330 cm^{-1} in the spectra of CMF and CMF film was weaker than that of the cellulose fibers due to the substitution of the hydroxyl group by the carboxylate group through carboxymethylation. Compared with that of the cellulose fibers, the spectrum of CMF had a strong absorption peak at 1593 cm^{-1}, and a small peak at 1410 cm^{-1}, which

corresponded to the presence of the COO^- [8]. Those bands provide evidence for the introduction of the carboxylate group on cellulose fibers.

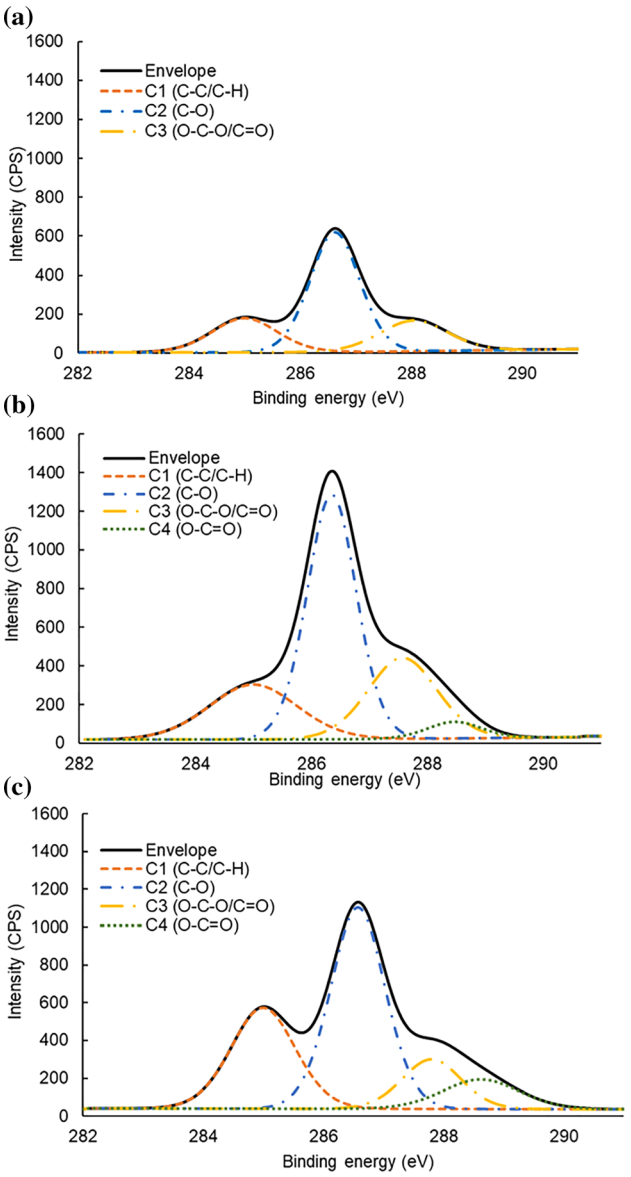

Figure 5 The high-resolution XPS C1*s* spectra of **a** Cellulose fibers, **b** CMF, and **c** CMF film.

When it comes to the CMF film, a new peak at 1720 cm^{-1}, which corresponded to the ester group, is evidence of the esterification of the CMF after the curing step [66]. The peak at 1367 cm^{-1} (–CH_3 symmetry deformation vibration) and 1234 cm^{-1} (C–O–C stretching vibration) were also the characteristics of the ester group, which also indicated the esterification occurred in the CMF film [67–69]. Furthermore, the weaker peak of the CMF film compared to CMF at 1593 cm^{-1} could be explained by the decrease in the carboxylate group of the CMF due to its esterification reaction of the hydroxyl group and carboxylate group of CMF.

The chemical structures of cellulose fibers, CMF, and CMF film were also studied using X-ray photoelectron spectrometry. The deconvolution of the C 1 s peak signal is represented in Fig. 5, the spectrum of cellulose fibers exhibited three peaks at 285 eV, 287.0 eV (ΔeV = 0.5 eV), and 288.4 eV (ΔeV = 0.6 eV) corresponding to C1 (C–C/C–H), C2 (C–O), and C3(O–C/C=O) bonds, respectively. The C1 signal is related to the contribution of non-oxidized alkane-type carbon atoms and impurities, or extractive compounds. The C2 signal is associated with the presence of ether groups originating from pure cellulose, as well as the hydroxyl groups of the unmodified cellulose, and the peak C3 presents the carbon connected to a carbonyl or two non-carbonyl oxygen atoms [70, 71]. The surface functional group compositions of the samples were calculated from XPS spectra (Fig. 5), and the results are available in Table 2. Also, a slight increase in the C3 peak intensity from 20.5 to 23.8% and a decrease in the C2 peak intensity from 57.5 to 51.4% were observed in the CMF spectrum (Table 2), which was probably the result of the substitution of hydroxyl groups due to the carboxymethylation. Moreover, a new peak C4 (binding energy at around 289 eV, ΔeV = 0.5 eV) was observed in the spectra of CMF and CMF film (Fig. 5b, c). An increase in the C4 peak from 3.9 to 10.1% was also observed in the spectrum of CMF film. These data imply that the hydroxyl groups were substituted by carboxyl groups after carboxymethylation and the formation of

Table 2 Surface functional groups compositions obtained by XPS analysis

Biomass	Relative atomic percentage (%) (C1*s* survey)			
	C1 (C–C/C–H)	C2 (C–O)	C3 (O–C–O/C=O)	C4 (O–C=O)
Cellulose fibers	21.9	57.5	20.5	ND*
CMF	21.0	51.4	23.8	3.9
CMF film	28.6	48.4	12.9	10.1

*Not detected

ester groups after film fabrication. According to Arun and coworkers, the C4 of the CMF spectrum is referred to as the carbon bound to a carbonyl and non-carbonyl oxygen [72, 73]. The decrease in the C2 and C3 peak intensities in the CMF spectrum might refer to the consumption of the hydroxyl group and carboxylate group due to esterification. In addition, an augment of C1 peak intensity from 21 to 28.6% in the CMF film (Table 2) might be attributed to the existence of acetic acid in the film originating from the film casting.

Mechanical properties of the crosslinked CMF films

Impact of carboxymethylated group

The tensile strength and Young's modulus of the CMF films are presented in Fig. 6. The CMF films have a tensile strength ranging from 18 to 60.8 MPa and Young's modulus ranging from 1.1 to 2.5 GPa. The tensile strength of CMF films increased with the augmented carboxylate group to 1.2 mmol/g. At a lower charge than 1.2 mmol/g, the carboxylate group probably widened the gaps between the bundles of cellulose fibers by introducing repulsive forces, facilitating the separation of the carboxymethylated cellulose fibers in the subsequent heating and stirring (i.e., curing) process [2]. Furthermore, the proportion of smaller fibers increased with the carboxylate group concentration on fibers (Fig. 2). These smaller cellulose fibers enhanced the entanglement between CMF and improved the contact area and potential bonding sites between CMF [12, 15, 74, 75]. In this case, the tensile strength of CMF films might be increased by the enhancement in the carboxymethylated group and thus entanglement of those fibrillated CMF (after heating and stirring) as seen in Fig. 6. As seen in Fig. 6a, however, the tensile strength of the CMF films decreased when the carboxylate group was changed from 1.2 to 1.4 mmol/g. This phenomenon can be explained by the reduction in the entanglement of carboxymethylated cellulose fibers [41, 76]. When the size of the fibers became very small (Fig. 1c), as a result of a substantial increase in the carboxylate group content, CMF may become weak and thin, which may decrease the entanglement between CMF reducing the tensile strength of the films [27, 74, 77, 78].

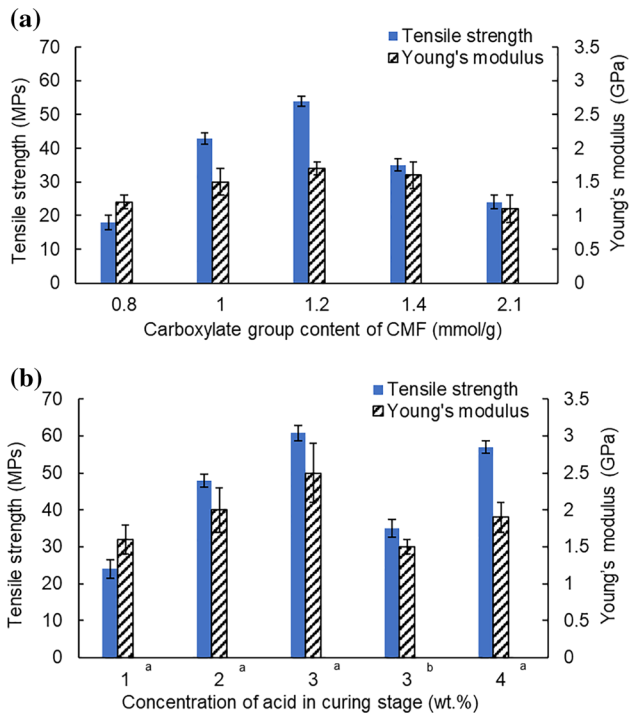

Figure 6 Tensile strength and Young's modulus for CMF film generated **a** from CMF with different carboxylate group contents, **b** via curing with different concentrations of acids, **a** Acetic acid **b** HCl.

Impact of acid in the curing process

Figure 6b shows the impact of acid concentration and type on the tensile strength and Young's modulus of CMF film. It is observable that the film generated with a 3 wt% acetic acid had the highest strength. The tensile strength of CMF film increased from 24 to 60.8 MPa when the amount of acetic acid raised from 1 to 3 wt%. The tensile decreased to 57 MPa when the acetic acid further increased to 4 wt%. This phenomenon could be explained by the function of acetic acid in esterification. As stated earlier, acetic acid functioned as a catalyst in the esterification of CMFs. Sahu and Pandit stated that the increased amount of catalyst would promote the crosslinking reaction contributing to the augment of the tensile strength of biofilm [41, 58]. However, Garavand and coworkers noted that some acids, e.g., citric acid, can not only involve in the crosslinking reaction but also act as a plasticizer in biofilm productions [37]. In the presence of extra acetic acid (> 3 wt%), the extra amount of acetic acid could act as a plasticizer and reduce the interactions between CMF macromolecules, which in turn would reduce the tensile strength of the crosslinked films. Similar results were reported by others

[79, 80], in which the tensile strength of starch-based biofilm was decreased by 10% when the content of citric acid was more than 3 wt%.

Compared to acetic acid, hydrochloric acid has less influence on the crosslinking reaction (Fig. 6b). The CMF film generated in the presence of HCl exhibited weaker tensile strength (35 MPa) than that generated in the presence of acetic acid (54 MPa) (Fig. 6b). A possible reason for this phenomenon could be the fact that HCl with the pKa of 1 might depolymerize/hydrolyze CMF during the film formation, decreasing the tensile strength of CMF [81]. Furthermore, Rojas and Azevedo stated that the mineral acid, such as nitric acid, can impair the tetraethoxysilane/cellulose composite matrix during the aging or drying period [57].

Considering the tensile strength results, the CMF film with 1.2 mmol/g carboxylate content was the best for fabricating the cellulose-based film. Also, a 3 wt% acetic acid that generated the CMF films with the highest tensile strength was selected as the most effective acid concentration for generating the CMF film.

Optical transmittance analysis

Figure 7 shows the transmittance of the CMF film as a function of wavelength. As seen, the more carboxylate group in the film, the higher transmittance of the film was obtained. The CMF film with 1.4 mmol/g carboxylate group content had a transmittance of approximately 48%. The CMF with 0.5 mmol/g carboxylate group content exhibited extremely low transparency (near 0%) and thus was not shown in the figure. The transparency of biofilm depends mainly on the size of the polymers used in biofilm production. The smaller the polymer, the weaker the light scattering and the higher the transparency of the biofilm would be [15, 82–84]. According to the result, the more carboxylate groups introduced to the CMF, the higher proportion of smaller cellulose fragments of CMF (Fig. 2) were used for the film generation, which improved the optical transmittance of the CMF films (Fig. 7). Meanwhile, the greater proportion of larger CMF fibers with a lower carboxylate group (0.8 mmol/g) (Fig. 2) could elevate the light scattering of the CMF films, which might be the reason for the low optical transmittance of the CMF film generated from CMF with 0.8 mmol/g carboxylate group (Fig. 7). Furthermore, the aggregation of long cellulose fibers can

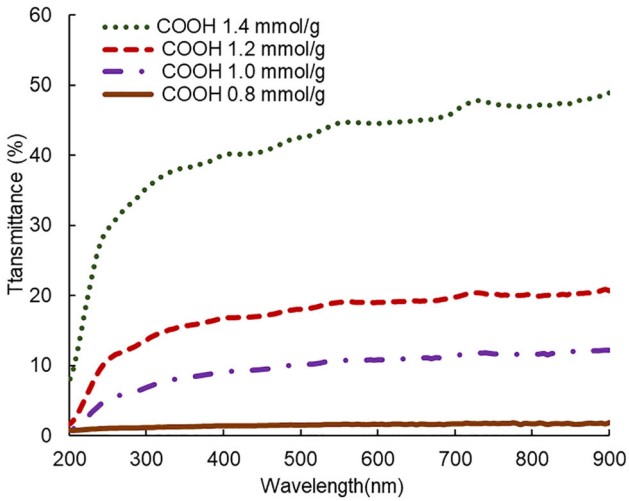

Figure 7 Optical transmittance of films generated in the presence of a 3 wt% acetic acid from the CMF with different carboxylate group contents.

lead to a dense layered structure in the film, increasing the light scattering of the film due to the strong interaction and van de Waals attraction between the fibers [15].

As stated previously, the transparency of biofilm was negatively affected by the size of cellulose fibers. The CMF film with the carboxylate group content of 1.4 mmol/g exhibited the highest transparency, whereas the one with less carboxylate group content (0.8 mmol/g) revealed low transparency (Figure S4 in the supplementary material). The morphology observation results showed the same tendency as the optical transmittance results (Figure S4 in the supplementary material). In this case, the SEM image revealed that the film with a lower carboxylate group content (0.8 mmol/g) exhibited lower transparency and more apparent fibrous structures (Figure S5). The aggregation performance of cellulose fibers was also observed in the SEM image. The white spot exhibited in the CMF film is evidence of the dense structure of cellulose fibers (Figure S4a). Thus, the optical transparency of CMF film was not as high as that of the PVA-based film reported in the literature with 90% transmittance in the range from 400 to 800 nm [85].

Water uptake performance of crosslinked CMF films

Figure 8 shows the water uptake performance of the CMF films. According to the data, the water uptake of the CMF films was increased from 1.84 to 4.80 g/g

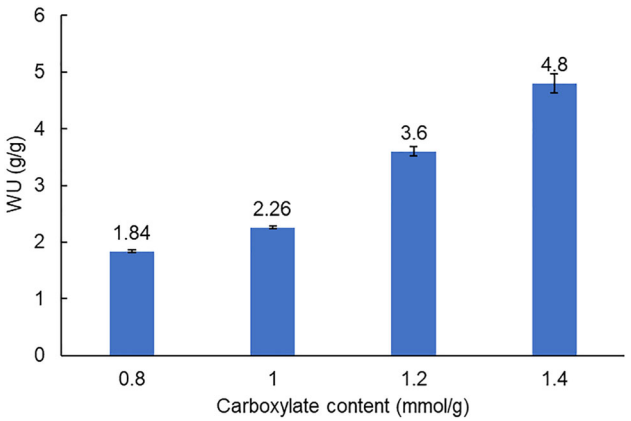

Figure 8 Water uptake of films generated in the presence of 3 wt% acetic acid from the CMF with different carboxylate group content.

when the carboxylate group content increased from 0.8 to 1.4 mmol/g. By adding more carboxylate groups to the film, the water absorption of the CMF film was increased, which is similar to what was reported previously [51, 86–88]. Furthermore, the existence of the carboxylate group contributed to the breakage of the hydrogen bonds, which improved the hydrophilicity of the CMF film [4, 89]. As Sabzalian stated, the possible reason for this behavior could be the esterification reaction between the carboxymethylated cellulose fibers in the CMF film [90]. Compared to other reports with the water uptake of 20 g/g, the CMF film in this study exhibited a lower water uptake capability, which implies its better water barrier properties [77, 91–95]. However, the water uptake performance of the CMF films was higher than some other polymeric composite films [96–100]. Water-resistance is an important characteristic of biofilms. A low water uptake (< 0.5 g/g) is required for the ideal biofilm production [96, 98, 100]. Thus, research on reducing the water uptake of CMF films needs to be undertaken. Interestingly, even though the CMF films contained high water uptake performance, the immersed CMF films didn't break during the test (Figure S6 in the supplementary material), which may be an attractive property for some applications, e.g., wound dressing.

Comparison of results

Table 3 exhibits tensile strength, optical transmittance, and water absorption of different biofilms produced in other studies. The tensile strength of cellulose/starch-based biofilm was in the range of 1–40 MPa. The biofilms with low tensile strength (below 10 MPa) seemed to have great optical transmittance. Among these biofilms, the highest water uptake was 2.27 g/g (and as low as 0.1 g/g) for the sample produced under 100% relative humidity (RH) at 20 °C [101–107].

The CMF film produced in this study exhibited an excellent tensile strength (up to 60.8 MPa) and optical transmittance in the range of 20% and 48%. Compared to those biofilms listed in Table 3, the CMF films fabricated in this study showed a relatively higher water uptake of 4.8 g/g than that reported by Lim et al. [103]. Thus, reducing the water uptake of the CMF films needs to be taken into account in future studies.

The good mechanical performance and acceptable transparency of the CMF film exhibit high potential in film packaging manufacturing. In opposition to other studies in which different methods of high shear stress fibrillation, such as high-pressure homogenization or ultrasonication, of cellulose fibers were used, cellulose fibers were slightly chemically treated in aqueous systems in this study, which would reduce the energy cost of the process [27, 108]. However, the relatively higher water uptake of the CMF film needs to be addressed to ensure its potential use in food packaging manufacturing.

Furthermore, the properties of packaging films proposed for food, pharmaceutical, and agriculture uses are listed in Table 3. It is seen that the tensile strength of those commercial plastics (3–60 MPa) is not very high. Interestingly, the CMF film reported in this study has a competitive tensile strength (60.8 MPa), which indicated that the CMF film has the potential to be used for those applications. On the other hand, for plant cultivations, low transmitting film may be more suitable to prevent the burning of plants from direct natural light [109]. For bag and pharmaceutical packaging, low light transmittance is also preferred. Therefore, one application of this film could be for packaging and agriculture uses [110, 111].

Conclusion

In this study, we prepared carboxymethylated cellulose fibers (CMFs) with low degrees of carboxymethylation. The primary emphasis of this work was on the evaluation of the physicochemical and

Table 3 Comparison of cellulose/starch-based biofilm and the properties of commercially available films used in the packaging industry

	Tensile strength (MPa)	Optical transmittance at 600 nm (%)	Water uptake (g/g)	Application	References
Biofilm/bioplastic					
CMF films	18–60.8	5–48	1.84–4.8	General applications	This work
Potato starch-based film blended with $CaCO_3$ nanoparticles	30–44	50–66	0.65–1.65	Food packaging, medical industries	[101]
Carboxymethyl cellulose based nano-biocomposites with graphene nano-platelets	3.44–7.74	15.69	0.24–0.59	Packaging	[102]
Cassava starch film plasticized with glycerol and sorbitol	1.77–30.3	76–81.04	0.10–0.26	Packaging	[103]
Papaya polysaccharide-corn starch film	3.03–4.86	74.26–88.77	~ 0.3	Food preservation	[104]
Cellulose nanofiber/bengkoang starch bio nanocomposites	10	43–80	0.15–0.2	Food packaging	[105]
Cellulose-based film modified by succinic anhydride	3.05–5.58	46.3–54.4	1.8–2.27	Biomedical field	[106]
Corn starch-based films incorporated with zanthoxylum bungeanum essential oil	1.23–3.89	76.4–84	0.23–0.34	Packaging	[107]
Commercial film products					
Novolen polypropylene	32–55	NR*	NR	Packaging	[112]
Nature works PLA	53–62	NR	NR	Dairy containers, food service ware	[112]
Dow ATTANE™ ultralow density polyethylene films	56.5	NR	NR	Sacks, plastic bags, mulch films, silage wrap	[113]
NOVA chemical SCLAIR® high-density polyethylene film	38–53	NR	NR	Food packaging	[113]
Arkema evatan ethylene–vinyl acetate copolymer polymer film	3–27	NR	NR	Rigid/flexible packaging in food, pharmaceuticals	[113]
NORTON® polytetrafluoroethylene film	7–22	NR	NR	Electrical application	[113]
SABIC innovative plastics Valox™ FR1 polybutylene terephthalate film	41.1	15%	NR	Packaging	[113]
MAKROFOL® DE 1-4 020209 polycarbonate	57.64	31%	NR	Signs and menu boards	[114]

*Not reported

mechanical properties of films made of carboxymethylated cellulose fibers with different degrees of carboxymethylation in the presence of acetic acid. The carboxymethylation and esterification reactions within the CMFs and CMF films were confirmed using FTIR, solid-state ^{13}C NMR, and XPS. It was observed that the high degree of carboxymethylation reduced the fiber length. The higher carboxymethylation tended to reduce the fiber size thus improving the optical properties of the films because smaller CMF in films could scatter light more effectively. However, it resulted in weaker mechanical properties of the film. On the other hand, the water uptake of the CMF film increased as the carboxymethylated group content of CMF increased since more hydrophilic functional groups were introduced to fibers via intensifying the carboxymethylation reaction. Also, a higher acetic acid content (e.g., 4 wt%) led to the augment of smaller CMF and increased the plasticity of the film, thus impairing the mechanical properties of the films. Furthermore, the CMF film produced in strong acid (HCl) exhibited a lower tensile strength than the one produced in the presence of acetic acid (35 MPa vs. 60.8 MPa), which might be due to the hydrolysis of cellulose fibers by HCl. The CMF films with the highest tensile strength of 60.8 MPa was achieved from the CMF with 1.2 mmol/g in the presence of 3 wt% acetic acid. The CMF films reported in this study exhibit competitive properties to the

commercial plastic film used in some applications (such as pharmaceuticals, electrical, and packaging). However, the high-water absorption of the CMF films (e.g., 4.8 g/g) should be addressed in future research.

Authors' contributions

YL contributed to raw data, method, concept, and first draft; NA contributed to concept, revisions, and analysis; PF contributed to revision and supervision.

Funding

The funding support of this work was provided by NSERC, Canada Foundation for Innovation, and Canada Research Chairs programs.

Availability of data and materials

Raw data of this work can be available upon request from the corresponding author.

Code availability

Not applicable.

Declarations

Conflict of interest The authors declare no conflict of interest, and all authors approved the publication of this paper.

Human or animal rights This article does not contain any studies with human participants or animals.

Supplementary Information: The online version contains supplementary material available at https://doi.org/10.1007/s10853-022-07262-0.

References

[1] Hosseinpour Feizi Z, Fatehi P (2020) Carboxymethylated cellulose nanocrystals as clay suspension dispersants: effect of size and surface functional groups. Cellulose 27(7):3759–3772. https://doi.org/10.1007/s10570-020-03024-w

[2] Sun B, Zhang M, Shen J, He Z, Fatehi P, Ni Y (2019) Applications of cellulose-based materials in sustained drug delivery systems. Curr Med Chem 26(14):2485–2501. https://doi.org/10.2174/0929867324666170705143308

[3] Hosseinpour Feizi Z, Fatehi P (2021) Interaction of hairy carboxyalkyl cellulose nanocrystals with cationic surfactant: effect of carbon spacer. Carbohydr Polym 255:117396. https://doi.org/10.1016/j.carbpol.2020.117396

[4] Yang G, Xia Y, Lin Z, Zhang K, Fatehi P, Chen J (2021) Physicochemical impact of cellulose nanocrystal on oxidation of starch and starch based composite films. Int J Biol Marcomol 184:42–49. https://doi.org/10.1016/j.ijbiomac.2021.06.009

[5] Zhao G, Lyu X, Lee J, Cui X, Chen WN (2019) Biodegradable and transparent cellulose film prepared ecofriendly from durian rind for packaging application. Food Packag Shelf Life 21:100345. https://doi.org/10.1016/j.fpsl.2019.100345

[6] Im W, Oh K, Abhari AR, Youn HJ, Lee HL (2019) Recycling of isopropanol for cost-effective, environmentally friendly production of carboxymethylated cellulose nanofibrils. Carbohydr Polym 208:365–371. https://doi.org/10.1016/j.carbpol.2018.12.093

[7] Paunonen S, Berthold F, Immonen K (2020) Poly (lactic acid)/pulp fiber composites: the effect of fiber surface modification and hydrothermal aging on viscoelastic and strength properties. J Appl Polym Sci 137:49617. https://doi.org/10.1002/app.49617

[8] Wang J, Dang M, Duan C, Zhao W, Wang K (2017) Carboxymethylated cellulose fibers as low-cost and renewable adsorbent materials. Ind Eng Chem Res 56:14940–14948. https://doi.org/10.1021/acs.iecr.7b03697

[9] Chen S, Wu M, Lu P, Gao L, Yan S, Wang S (2020) Development of pH indicator and antimicrobial cellulose nanofibre packaging film based on purple sweet potato anthocyanin and oregano essential oil. Int J Biol Macromol 149:271–280. https://doi.org/10.1016/j.ijbiomac.2020.01.231

[10] Orelma H, Hokkanen A, Leppänen I, Kammiovirta K, Kapulainen M, Harlin A (2020) Optical cellulose fiber made from regenerated cellulose and cellulose acetate for water sensor applications. Cellulose 27:1543–1553. https://doi.org/10.1007/s10570-019-02882-3

[11] Suwanprateep S, Kumsapaya C, Sayan P (2019) Structure and thermal properties of rice starch-based film blended with mesocarp cellulose fiber. Mater Today Proc 17:2039–2047. https://doi.org/10.1016/j.matpr.2019.06.252

[12] Kalia S, Boufi S, Celli A, Kango S (2014) Nanofibrillated cellulose: surface modification and potential applications.

Colloid Polym Sci 292:5–31. https://doi.org/10.1007/s00396-013-3112-9

[13] Nechyporchuk O, Pignon F, Belgacem MN (2015) Morphological properties of nanofibrillated cellulose produced using wet grinding as an ultimate fibrillation process. J Mater Sci 50:531–541. https://doi.org/10.1007/s10853-014-8609-1

[14] Khalil HA, Davoudpour Y, Islam MN, Mustapha A, Sudesh K, Dungani R, Jawaid M (2014) Production and modification of nanofibrillated cellulose using various mechanical processes: a review. Carbohydr Polym 99:649–665. https://doi.org/10.1016/j.carbpol.2013.08.069

[15] Barbash VA, Yaschenko OV, Alushkin SV, Kondratyuk AS, Posudievsky OY, Koshechko VG (2016) The effect of mechanochemical treatment of the cellulose on characteristics of nanocellulose films. Nanoscale Res Lett 11:1–8. https://doi.org/10.1186/s11671-016-1632-1

[16] He M, Yang G, Cho BU, Lee YK, Won JM (2017) Effects of addition method and fibrillation degree of cellulose nanofibrils on furnish drainability and paper properties. Cellulose 24:5657–5669. https://doi.org/10.1007/s10570-017-1495-3

[17] Bisht SS, Pandey KK, Joshi G, Naithani S (2017) New route for carboxymethylation of cellulose: synthesis, structural analysis and properties. Cellul Chem Technol 51:609–617

[18] Haleem N, Arshad M, Shahid M, Tahir MA (2014) Synthesis of carboxymethyl cellulose from waste of cotton ginning industry. Carbohydr Polym 113:249–255. https://doi.org/10.1016/j.carbpol.2014.07.023

[19] Heinze T, Koschella A (2005) Carboxymethyl ethers of cellulose and starch–a review. Macromol Symp 233:13–40. https://doi.org/10.1002/masy.200550502

[20] Heydarzadeh HD, Najafpour GD, Nazari-Moghaddam AA (2009) Catalyst-free conversion of alkali cellulose to fine carboxymethyl cellulose at mild conditions. World Appl Sci J 6:564–569

[21] Joshi G, Naithani S, Varshney VK, Bisht SS, Rana V, Gupta PK (2015) Synthesis and characterization of carboxymethyl cellulose from office waste paper: a Greener approach towards waste management. Waste Manag 38:33–40. https://doi.org/10.1016/j.wasman.2014.11.015

[22] Pushpamalar V, Langford SJ, Ahmad M, Lim YY (2006) Optimization of reaction conditions for preparing carboxymethyl cellulose from sago waste. Carbohydr Polym 64:312–318. https://doi.org/10.1016/j.carbpol.2005.12.003

[23] dos Santos DM, de Lacerda BA, Ascheri DPR, Signini R, de Aquino GLB (2015) Microwave-assisted carboxymethylation of cellulose extracted from Brewer's spent grain. Carbohydr Polym 131:125–133. https://doi.org/10.1016/j.carbpol.2015.05.051

[24] Yeasmin MS, Mondal MIH (2015) Synthesis of highly substituted carboxymethyl cellulose depending on cellulose particle size. Int J Biol Macromol 80:725–731. https://doi.org/10.1016/j.ijbiomac.2015.07.040

[25] Rol F, Belgacem MN, Gandini A, Bras J (2019) Recent advances in surface-modified cellulose nanofibrils. Prog Polym Sci 88:241–264. https://doi.org/10.1016/j.progpolymsci.2018.09.002

[26] Abushammala H, Mao J (2019) A review of the surface modification of cellulose and nanocellulose using aliphatic and aromatic mono-and di-isocyanates. Molecules 24:2782. https://doi.org/10.3390/molecules24152782

[27] Luo J, Zhang M, Yang B, Liu G, Tan J, Nie J, Song S (2019) A promising transparent and UV-shielding composite film prepared by aramid nanofibers and nanofibrillated cellulose. Carbohydr Polym 203:110–118. https://doi.org/10.1016/j.carbpol.2018.09.040

[28] Bedane AH, Eić M, Farmahini-Farahani M, Xiao H (2015) Water vapor transport properties of regenerated cellulose and nanofibrillated cellulose films. J Membr Sci 493:46–57. https://doi.org/10.1016/j.memsci.2015.06.009

[29] Nunes MR, Castilho MDSM, de Lima Veeck AP, da Rosa CG, Noronha CM, Maciel MV, Barreto PM (2018) Antioxidant and antimicrobial methylcellulose films containing Lippia alba extract and silver nanoparticles. Carbohydr Polym 192:37–43. https://doi.org/10.1016/j.carbpol.2018.03.014

[30] Borges JP, Godinho MH, Martins AF, Stamatialis DF, De Pinho MN, Belgacem MN (2004) Tensile properties of cellulose fiber reinforced hydroxypropylcellulose films. Polym Compos 25:102–110. https://doi.org/10.1002/pc.20008

[31] Villalobos R, Chanona J, Hernández P, Gutiérrez G, Chiralt A (2005) Gloss and transparency of hydroxypropyl methylcellulose films containing surfactants as affected by their microstructure. Food Hydrocoll 19:53–61. https://doi.org/10.1016/j.foodhyd.2004.04.014

[32] Cazón P, Velazquez G, Ramírez JA, Vázquez M (2017) Polysaccharide-based films and coatings for food packaging: a review. Food Hydrocoll 68:136–148. https://doi.org/10.1016/j.foodhyd.2016.09.009

[33] Kumar N, Neeraj, (2019) Polysaccharide-based component and their relevance in edible film/coating: a review. Nutr Food Sci 49:793–823. https://doi.org/10.1108/NFS-10-2018-0294

[34] Oun AA, Rhim JW (2015) Preparation and characterization of sodium carboxymethyl cellulose/cotton linter cellulose

nanofibril composite films. Carbohydr Polym 127:101–109. https://doi.org/10.1016/j.carbpol.2015.03.073

[35] Paunonen S (2013) Strength and barrier enhancements of cellophane and cellulose derivative films: a review. BioResources 8(2):3098–3121

[36] Shahbazi M, Ahmadi SJ, Seif A, Rajabzadeh G (2016) Carboxymethyl cellulose film modification through surface photo-crosslinking and chemical crosslinking for food packaging applications. Food Hydrocoll 61:378–389. https://doi.org/10.1016/j.foodhyd.2016.04.021

[37] Garavand F, Rouhi M, Razavi SH, Cacciotti I, Mohammadi R (2017) Improving the integrity of natural biopolymer films used in food packaging by crosslinking approach: a review. Int J Biol Macromol 104:687–707. https://doi.org/10.1016/j.ijbiomac.2017.06.093

[38] Rouhi M, Razavi SH, Mousavi SM (2017) Optimization of crosslinked poly (vinyl alcohol) nanocomposite films for mechanical properties. Mater Sci Eng C 71:1052–1063. https://doi.org/10.1016/j.msec.2016.11.135

[39] Šešlija S, Nešić A, Škorić ML, Krušić MK, Santagata G, Malinconico M (2018) Pectin/carboxymethylcellulose films as a potential food packaging material. Macromol Symp 378:1600163. https://doi.org/10.1002/masy.201600163

[40] Tang A, Yan C, Li D, Chen S (2018) Acid-catalyzed crosslinking of cellulose nanofibers with glutaraldehyde to improve the water resistance of nanopaper. J Bioresour Bioprod 3:59–64. https://doi.org/10.21967/jbb.v3i2.97

[41] Azeredo HM, Waldron KW (2016) Crosslinking in polysaccharide and protein films and coatings for food contact—a review. Trends Food Sci Technol 52:109–122. https://doi.org/10.1016/j.tifs.2016.04.008

[42] Borůvková K, Wiener J, Kukreja S (2012) Thermal self crosslinking of carboxymethylcellulose. ACC J XVIII/1, 6–13

[43] Fan J, Zhang S, Li F, Yang Y, Du M (2020) Recent advances in cellulose-based membranes for their sensing applications. Cellulose 27:1–23. https://doi.org/10.1007/s10570-020-03445-7

[44] Hassan SH, Voon LH, Velayutham TS, Zhai L, Kim HC, Kim J (2018) Review of cellulose smart material: biomass conversion process and progress on cellulose-based electroactive paper. J Renew Mater 6:1–25. https://doi.org/10.7569/JRM.2017.634173

[45] Santos RF, Ribeiro JCL, de Carvalho JMF, Magalhães WLE, Pedroti LG, Nalon GH, de Lima GES (2021) Nanofibrillated cellulose and its applications in cement-based composites: a review. Constr Build Mater 288:123122. https://doi.org/10.1016/j.conbuildmat.2021.123122

[46] Yang H, Tejado A, Alam N, Antal M, van de Ven TG (2012) Films prepared from electrostatically stabilized nanocrystalline cellulose. Langmuir 28(20):7834–7842. https://doi.org/10.1021/la2049663

[47] Fechter C, Heinze T (2019) Influence of wood pulp quality on the structure of carboxymethyl cellulose. J Appl Polym Sci 136:47862. https://doi.org/10.1002/app.47862

[48] Osong SH, Norgren S, Engstrand P (2016) Processing of wood-based microfibrillated cellulose and nanofibrillated cellulose, and applications relating to papermaking: a review. Cellulose 23:93–123. https://doi.org/10.1007/s10570-015-0798-5

[49] Im W, Lee S, Abhari AR, Youn HJ, Lee HL (2018) Optimization of carboxymethylation reaction as a pretreatment for production of cellulose nanofibrils. Cellulose 25:3873–3883. https://doi.org/10.1007/s10570-018-1853-9

[50] Ismail NM, Bono A, Valintinus ACR, Nilus S, Chng LM (2010) Optimization of reaction conditions for preparing carboxymethyl cellulose. J Appl Sci 10:2530–2536

[51] Chen JH, Liu JG, Su YQ, Xu ZH, Li MC, Ying RF, Wu JQ (2019) Preparation and properties of microfibrillated cellulose with different carboxyethyl content. Carbohydr Polym 206:616–624. https://doi.org/10.1016/j.carbpol.2018.11.024

[52] Naderi A, Lindström T, Erlandsson J, Sundström J, Flodberg G (2016) A comparative study of the properties of three nano-fibrillated cellulose systems that have been produced at about the same energy consumption levels in the mechanical delamination step. Nordic Pulp Pap Res J 31:364–371. https://doi.org/10.3183/npprj-2016-31-03-p364-371

[53] Naderi A, Lindström T, Pettersson T (2014) The state of carboxymethylated nanofibrils after homogenization-aided dilution from concentrated suspensions: a rheological perspective. Cellulose 21:2357–2368. https://doi.org/10.1007/s10570-014-0329-9

[54] Su L, Ou Y, Feng X, Lin M, Li J, Liu D, Qi H (2019) Integrated production of cellulose nanofibers and sodium carboxymethylcellulose through controllable eco-carboxymethylation under mild conditions. ACS Sustain Chem Eng 7:3792–3800. https://doi.org/10.1021/acssuschemeng.8b04492

[55] Xie H, Du H, Yang X, Si C (2018) Recent strategies in preparation of cellulose nanocrystals and cellulose nanofibrils derived from raw cellulose materials. Int J Polym Sci 2018:7923068. https://doi.org/10.1155/2018/7923068

[56] Wang Y, Wang X, Xie Y, Zhang K (2018) Functional nanomaterials through esterification of cellulose: a review

of chemistry and application. Cellulose 25:3703–3731. https://doi.org/10.1007/s10570-018-1830-3

[57] Rojas J, Azevedo E (2011) Functionalization and crosslinking of microcrystalline cellulose in aqueous media: a safe and economic approach. Int J Pharma Sci Rev Res 8:28–36

[58] Sahu A, Pandit AB (2019) Kinetic study of homogeneous catalyzed esterification of a series of aliphatic acids with different alcohols. Ind Eng Chem Res 58:2672–2682. https://doi.org/10.1021/acs.iecr.8b04781

[59] Ghorpade VS, Dias RJ, Mali KK, Mulla SI (2019) Citric acid crosslinked carboxymethylcellulose-polyvinyl alcohol hydrogel films for extended release of water soluble basic drugs. J Drug Deliv Sci Technol 52:421–430. https://doi.org/10.1016/j.jddst.2019.05.013

[60] Reddy KO, Maheswari CU, Dhlamini MS, Mothudi BM, Zhang J, Zhang J, Rajulu AV (2017) Preparation and characterization of regenerated cellulose films using borassus fruit fibers and an ionic liquid. Carbohydr Polym 160:203–211. https://doi.org/10.1016/j.carbpol.2016.12.051

[61] Tang R, Yu Z, Renneckar S, Zhang Y (2018) Coupling chitosan and TEMPO-oxidized nanofibrilliated cellulose by electrostatic attraction and chemical reaction. Carbohydr Polym 202:84–90. https://doi.org/10.1016/j.carbpol.2018.08.097

[62] Abouloula CN, Rizwan M, Selvanathan V, Abdullah CI, Hassan A, Yahya R, Oueriagli A (2018) A novel application for oil palm empty fruit bunch: extraction and modification of cellulose for solid polymer electrolyte. Ionics 24:3827–3836. https://doi.org/10.1007/s11581-018-2558-7

[63] Guo T, Gu L, Zhang Y, Chen H, Jiang B, Zhao H, Xiao H (2019) Bioinspired self-assembled films of carboxymethyl cellulose–dopamine/montmorillonite. J Mat Chem A 7:14033–14041. https://doi.org/10.1039/C9TA00998A

[64] Kong X, Zhang S, Wang Y, Liu Y, Li R, Ren X, Huang TS (2019) Antibacterial polyvinyl alcohol films incorporated with N-halamine grafted oxidized microcrystalline cellulose. Compos Commun 15:25–29. https://doi.org/10.1016/j.coco.2019.06.005

[65] Vuoti S, Laatikainen E, Heikkinen H, Johansson LS, Saharinen E, Retulainen E (2013) Chemical modification of cellulosic fibers for better convertibility in packaging applications. Carbohydr Polym 96:549–559. https://doi.org/10.1016/j.carbpol.2012.07.053

[66] Yang CQ (1991) FT-IR spectroscopy study of the ester crosslinking mechanism of cotton cellulose. Text Res J 61:433–440. https://doi.org/10.1177/004051759106100801

[67] Abe M, Enomoto Y, Seki M, Miki T (2020) Esterification of solid wood for plastic forming. BioResour 15:6282–6298

[68] Lu K, Zhu J, Bao X, Liu H, Yu L, Chen L (2020) Effect of starch microstructure on microwave-assisted esterification. Int J Biol Macromol 164:2550–2557. https://doi.org/10.1016/j.ijbiomac.2020.08.099

[69] Oun AA, Rhim JW (2016) Isolation of cellulose nanocrystals from grain straws and their use for the preparation of carboxymethyl cellulose-based nanocomposite films. Carbohydr Polym 150:187–200. https://doi.org/10.1016/j.carbpol.2016.05.020

[70] Chen Y, Long Y, Li Q, Chen X, Xu X (2019) Synthesis of high-performance sodium carboxymethyl cellulose-based adsorbent for effective removal of methylene blue and Pb (II). Int J Biol Macromol 126:107–117. https://doi.org/10.1016/j.ijbiomac.2018.12.119

[71] Le Gars M, Roger P, Belgacem N, Bras J (2020) Role of solvent exchange in dispersion of cellulose nanocrystals and their esterification using fatty acids as solvents. Cellulose 27:4319–4336. https://doi.org/10.1007/s10570-020-03101-0

[72] Arun V, Perumal EM, Prakash KA, Rajesh M, Tamilarasan K (2020) Sequential fractionation and characterization of lignin and cellulose fiber from waste rice bran. J Environ Chem Eng 8:104124. https://doi.org/10.1016/j.jece.2020.104124

[73] Leszczyńska A, Radzik P, Szefer E, Mičušík M, Omastova M, Pielichowski K (2019) Surface modification of cellulose nanocrystals with succinic anhydride. Polymers 11:866. https://doi.org/10.3390/polym11050866

[74] Lin C, Wang Q, Deng Q, Huang H, Huang F, Huang L, Ma X (2019) Preparation of highly hazy transparent cellulose film from dissolving pulp. Cellulose 26:4061–4069. https://doi.org/10.1007/s10570-019-02367-3

[75] Liu W, Mohanty AK, Askeland P, Drzal LT, Misra M (2004) Influence of fiber surface treatment on properties of Indian grass fiber reinforced soy protein based biocomposites. Polymers 45:7589–7596. https://doi.org/10.1016/j.polymer.2004.09.009

[76] Li W, Wang S, Wang W, Qin C, Wu M (2019) Facile preparation of reactive hydrophobic cellulose nanofibril film for reducing water vapor permeability (WVP) in packaging applications. Cellulose 26:3271–3284. https://doi.org/10.1007/s10570-019-02270-x

[77] Gadhave RV, Das A, Mahanwar PA, Gadekar PT (2018) Starch based bio-plastics: the future of sustainable packaging. Open J Polym Chem 8:21–33. https://doi.org/10.4236/ojpchem.2018.82003

[78] Sim G, Liu Y, van de Ven T (2016) Transparent composite films prepared from chemically modified cellulose fibers. Cellulose 23:2011–2024. https://doi.org/10.1007/s10570-016-0923-0

[79] Ghanbarzadeh B, Almasi H, Entezami AA (2011) Improving the barrier and mechanical properties of corn-starch-based edible films: effect of citric acid and carboxymethyl cellulose. Ind Crop Prod 33:229–235. https://doi.org/10.1016/j.indcrop.2010.10.016

[80] Ning W, Jiugao Y, Xiaofei M, Ying W (2007) The influence of citric acid on the properties of thermoplastic starch/linear low-density polyethylene blends. Carbohydr Polym 67:446–453. https://doi.org/10.1016/j.carbpol.2006.06.014

[81] Kang IS, Yang CQ, Wei W, Lickfield GC (1998) Mechanical strength of durable press finished cotton fabrics: part I: effects of acid degradation and crosslinking of cellulose by polycarboxylic acids. Text Res J 68:865–870. https://doi.org/10.1177/004051759806801112

[82] Nogi M, Iwamoto S, Nakagaito AN, Yano H (2009) Optically transparent nanofiber paper. Adv Mater 21:1595–1598. https://doi.org/10.1002/adma.200803174

[83] Saito T, Kimura S, Nishiyama Y, Isogai A (2007) Cellulose nanofibers prepared by TEMPO-mediated oxidation of native cellulose. Biomacromol 8:2485–2491. https://doi.org/10.1021/bm0703970

[84] Sun X, Wu Q, Zhang X, Ren S, Lei T, Li W, Zhang Q (2018) Nanocellulose films with combined cellulose nanofibers and nanocrystals: tailored thermal, optical and mechanical properties. Cellulose 25:1103–1115. https://doi.org/10.1007/s10570-017-1627-9

[85] Cai J, Chen J, Zhang Q, Lei M, He J, Xiao A, Xiong H (2016) Well-aligned cellulose nanofiber-reinforced polyvinyl alcohol composite film: mechanical and optical properties. Carbohydr Polym 140:238–245. https://doi.org/10.1016/j.carbpol.2015.12.039

[86] Cuadri AA, Romero A, Bengoechea C, Guerrero A (2018) The effect of carboxyl group content on water uptake capacity and tensile properties of functionalized soy protein-based superabsorbent plastics. J Polym Environ 26:2934–2944. https://doi.org/10.1007/s10924-018-1183-x

[87] Poussard L, Burel F, Couvercelle JP, Merhi Y, Tabrizian M, Bunel C (2004) Hemocompatibilty of new ionic polyurethanes: influence of carboxylic group insertion modes. Biomaterials 25:3473–3483. https://doi.org/10.1016/j.biomaterials.2003.10.069

[88] Sim G (2016) Carboxylated cellulose pulp fibers: from fundamentals to applications. Dissertation, McGill University

[89] Tosh B (2014) Synthesis and sustainable applications of cellulose esters and ethers: a review. Intl J Energy Sustain Env Eng 1:56–78

[90] Sabzalian Z (2012) Cross-linking and hydrophobization of chemically modified cellulose fibers. Dissertation, McGill University

[91] Basu P, Narendrakumar U, Arunachalam R, Devi S, Manjubala I (2018) Characterization and evaluation of carboxymethyl cellulose-based films for healing of full-thickness wounds in normal and diabetic rats. ACS Omega 3:12622–12632. https://doi.org/10.1021/acsomega.8b02015

[92] Goetz L, Mathew A, Oksman K, Gatenholm P, Ragauskas AJ (2009) A novel nanocomposite film prepared from crosslinked cellulosic whiskers. Carbohydr Polym 75:85–89. https://doi.org/10.1016/j.carbpol.2008.06.017

[93] Kanafi NM, Rahman NA, Rosdi NH (2019) Citric acid cross-linking of highly porous carboxymethyl cellulose/poly (ethylene oxide) composite hydrogel films for controlled release applications. Mater Today Proc 7:721–731. https://doi.org/10.1016/j.matpr.2018.12.067

[94] Kowalczyk D, Pytka M, Szymanowska U, Skrzypek T, Łupina K, Biendl M (2020) Release kinetics and antibacterial activity of potassium salts of iso-α-acids loaded into the films based on gelatin, carboxymethyl cellulose and their blends. Food Hydrocoll 109:106104. https://doi.org/10.1016/j.foodhyd.2020.106104

[95] Wang W, Zhang X, Li C, Du G, Zhang H, Ni Y (2018) Using carboxylated cellulose nanofibers to enhance mechanical and barrier properties of collagen fiber film by electrostatic interaction. J Sci Food Agric 98:3089–3097. https://doi.org/10.1002/jsfa.8809

[96] Biddeci G, Cavallaro G, Di Blasi F, Lazzara G, Massaro M, Milioto S, Spinelli G (2016) Halloysite nanotubes loaded with peppermint essential oil as filler for functional biopolymer film. Carbohydr Polym 152:548–557. https://doi.org/10.1016/j.carbpol.2016.07.041

[97] Castro PM, Fonte P, Oliveira A, Madureira AR, Sarmento B, Pintado ME (2017) Optimization of two biopolymer-based oral films for the delivery of bioactive molecules. Mater Sci Eng C 76:171–180. https://doi.org/10.1016/j.msec.2017.02.173

[98] Condés MC, Añón MC, Dufresne A, Mauri AN (2018) Composite and nanocomposite films based on amaranth biopolymers. Food Hydrocoll 74:159–167. https://doi.org/10.1016/j.foodhyd.2017.07.013

[99] Rivadeneira J, Audisio MC, Gorustovich A (2018) Films based on soy protein-agar blends for wound dressing: Effect of different biopolymer proportions on the drug release rate and the physical and antibacterial properties of

the films. J Biomater Appl 32:1231–1238. https://doi.org/10.1177/0885328218756653

[100] Sultan NFK, Johari WLW (2017) The development of banana peel/corn starch bioplastic film: a preliminary study. Bioremediat Sci Technol Res 5:12–17. https://doi.org/10.54987/bstr.v5i1.352

[101] Dawale SA, Bhagat MM (2018) Preparation and characterization of potato starch based film blended with CaCo3 nanoparticles. Int J Eng Sci 8:16013–16016

[102] Ebrahimzadeh S, Ghanbarzadeh B, Hamishehkar H (2016) Physical properties of carboxymethyl cellulose based nanobiocomposites with Graphene nano-platelets. Int J Biol Macromol 84:16–23. https://doi.org/10.1016/j.ijbiomac.2015.11.074

[103] Lim WS, Ock SY, Park GD, Lee IW, Lee MH, Park HJ (2020) Heat-sealing property of cassava starch film plasticized with glycerol and sorbitol. Food Packag Shelf Life 26:100556. https://doi.org/10.1016/j.fpsl.2020.100556

[104] Ma Y, Zhao Y, Xie J, Sameen DE, Ahmed S, Dai J, Liu Y (2020) Optimization, characterization and evaluation of papaya polysaccharide-corn starch film for fresh cut apples. Int J Biol Macromol 166:1057–1071. https://doi.org/10.1016/j.ijbiomac.2020.10.261

[105] Mahardika M, Abral H, Kasim A, Arief S, Hafizulhaq F, Asrofi M (2019) Properties of cellulose nanofiber/bengkoang starch bionanocomposites: effect of fiber loading. Lwt 116:108554. https://doi.org/10.1016/j.lwt.2019.108554

[106] Shi C, Tao F, Cui Y (2018) Cellulose-based film modified by succinic anhydride for the controlled release of domperidone. J Biomater Sci Polym Ed 29:1233–1249. https://doi.org/10.1080/09205063.2018.1456024

[107] Wang B, Sui J, Yu B, Yuan C, Guo L, Abd El-Aty AM, Cui B (2020) Physicochemical properties and antibacterial activity of corn starch-based films incorporated with *Zanthoxylum bungeanum* essential oil. Carbohydr Polym 254:117314. https://doi.org/10.1016/j.carbpol.2020.117314

[108] Mandal A, Chakrabarty D (2019) Studies on mechanical, thermal, and barrier properties of carboxymethyl cellulose film highly filled with nanocellulose. J Thermoplast Compos Mater 32:995–1014. https://doi.org/10.1177/0892705718772868

[109] Espi E, Salmeron A, Fontecha A, García Y, Real AI (2006) Plastic films for agricultural applications. J Plast Film Sheeting 22:85–102. https://doi.org/10.1177/8756087906064220

[110] He G, Wang Z, Hui X, Huang T, Luo L (2021) Black film mulching can replace transparent film mulching in crop production. Field Crop Res 261:108026. https://doi.org/10.1016/j.fcr.2020.108026

[111] Pardos F (2004) Plastic films: situation and outlook: a Rapra market report. iSmithers Rapra Publishing, UK

[112] Ebnesajjad S (ed) (2012) Plastic films in food packaging: materials, technology and applications. William Andrew, Oxford

[113] McKeen LW (2017) Film properties of plastics and elastomers, 4th edn. William Andrew, Oxford

[114] Coverstro (2012) Technical Data Sheets for MAKROFOL® DE 1–4 020209 film. https://www.curbellplastics.com/Research-Solutions/Technical-Resources/Technical-Resources/Makrofol-DE-1-4-020209